

NNLO QCD corrections to the q^2 spectrum of inclusive semileptonic B -meson decays

MATTEO FAEL^a AND FLORIAN HERREN^b

^a *Theoretical Physics Department, CERN, 1211 Geneva, Switzerland*

^b *Physics Institute, Universität Zürich, Winterthurerstrasse 190, CH-8057 Zürich, Switzerland*

Abstract

We calculate the next-to-next-to-leading order QCD corrections to the leptonic invariant mass (q^2) spectrum of semileptonic $b \rightarrow c$ inclusive decays, taking into account the mass of the charm quark and the charged lepton in the final state. We obtain analytic results in terms of generalized polylogarithms and present numerical studies of the $\mathcal{O}(\alpha_s^2)$ corrections to the q^2 spectrum of $b \rightarrow c\ell\bar{\nu}_\ell$ decays, for $\ell = e, \mu$ and τ , in the kinetic scheme. Our computation can be used to incorporate the recent measurements of q^2 moments by Belle and Belle II into global fits of inclusive semileptonic B -decays.

1 Introduction

The Heavy Quark Expansion (HQE) has become a pillar in the theoretical description of inclusive decays of heavy hadrons, allowing the derivation of precise predictions with reliable estimates of the uncertainties. One of its main applications is the study of the inclusive decay $B \rightarrow X_c \ell \bar{\nu}_\ell$. Thanks to its relatively large rate and clean experimental signature, studies of inclusive semileptonic decays have led to precise determinations of the magnitude of the Cabibbo-Kobayashi-Maskawa matrix element V_{cb} .

The HQE allows to describe both the total decay rate and various kinematic distributions as a double series expansions in the strong coupling constant α_s and Λ_{QCD}/m_b . Various measurements of moments of the charged lepton energy and the hadronic invariant mass in $B \rightarrow X_c \ell \bar{\nu}_\ell$ decays have been performed by BABAR [1,2], BELLE [3,4], CLEO [5], CDF [6] and DELPHI [7]. The comparison of experimental measurements with the predictions calculated within the HQE has led to determinations of $|V_{cb}|$ with a 1.1% accuracy [8–10] and the so called “HQE parameters”, the non-perturbative matrix elements, such as $\mu_\pi^2, \mu_G^2, \rho_D^3$ and ρ_{LS} .

The HQE parameters are important theoretical inputs not only for the extraction of $|V_{cb}|$, but also for the extraction of $|V_{ub}|$ from $B \rightarrow X_u \ell \bar{\nu}_\ell$ decays since the moments of the shape functions can be related to the HQE parameters extracted in $b \rightarrow c$ decays. Moreover predictions for other kinds of processes require precise knowledge of the HQE parameters, as for instance the B -meson lifetimes [11,12] and the rare decay $B \rightarrow X_{d,s} \ell \bar{\ell}$ [13,14].

An alternative method for the determination of $|V_{cb}|$ has been proposed in Ref. [15] and is based on the measurement of the leptonic invariant mass (q^2) spectrum and the branching ratio as a function of a lower cut on q^2 . These observables are invariant under reparametrization, a symmetry within the HQE reflecting Lorentz invariance of the underlying QCD. Reparametrization invariant (RPI) quantities depend on a reduced set of HQE parameters [15,16]. The smaller set of parameters necessary in a global fit of these observables (eight instead of 13 up to $1/m_b^4$) enabled to extract $|V_{cb}|$ and the HQE parameters up to $1/m_b^4$ in a completely data-driven way [17], based on recent measurements of q^2 moments by Belle [18] and Belle-II [19]. The new measurements of the q^2 moments have also been included in a global fit of $|V_{cb}|$ [10], together with the lepton energy and M_X moments, finding that the new data are compatible with the other measurements and slightly decreasing the uncertainty on the HQE parameters and on $|V_{cb}|$. Recently, the RPI operator basis has been extended up to order $1/m_b^5$ [20].

Given the precision achieved by experimental measurements, which show a percent or even sub-percent relative accuracy for certain observables, a good control of perturbative and non-perturbative effects in the HQE is mandatory, also in light of the rather large value of the strong coupling constant $\alpha_s(m_b) \simeq 0.22$. At the partonic level, next-to-leading order (NLO) corrections are available from Ref. [21–23]. The $\mathcal{O}(\alpha_s)$ triple differential distribution up to the power-suppressed terms μ_π^2 and μ_G^2 were presented in Ref. [24–26], while NLO corrections proportional to ρ_D are available only for the total rate and the q^2 spectrum [27].

The $\mathcal{O}(\alpha_s^2)$ corrections to the free quark decay $b \rightarrow X_c \ell \bar{\nu}_\ell$ are also required for a consistent theoretical description and to match the experimental accuracy. The next-to-next-

to-leading order (NNLO) corrections to the hadronic invariant mass and charged-lepton energy moments have been calculated in [28, 29]. No result is available for the q^2 spectrum for arbitrary values of q^2 , only for $q^2 = 0$ [30], $q^2 = (m_b - m_c)^2$ [31, 32] and $q^2 = m_c^2$ [33]. While the calculations in these three special points allowed the authors of Ref. [33] to estimate the non-BLM corrections at $\mathcal{O}(\alpha_s^2)$ with a relative 30% uncertainty, their result is unsuited to calculate higher moments of the q^2 spectrum with sufficient precision.¹ Analytic expressions up to $\mathcal{O}(\alpha_s^3)$ for the q^2 moments without threshold selection cuts have been presented in Ref. [34], while Ref. [10] presented an evaluation of the $\alpha_s^2\beta_0$ corrections, utilizing the BLM correction to the triple differential rate from Ref. [23].

The goal of this paper is to present the complete NNLO QCD corrections to the q^2 spectrum of $b \rightarrow X_c \ell \bar{\nu}_\ell$. At variance with the numerical approach used in [28, 29], based on sector decomposition, recent developments in analytic approaches to multi-loop computations allow us to calculate the differential rate w.r.t. q^2 in an analytic form and write it in terms of generalized polylogarithms (GPLs) [35, 36]. Our results can be used to calculate the NNLO corrections to the q^2 moments with arbitrary cuts on q^2 . The inclusion of the results presented in this paper into global fits will allow to better assess the theoretical uncertainty in the prediction.

The paper is organized as follows. In Section 2 we present the details of the calculation, in particular we discuss how we obtain analytic results for the three-loop master integrals at NNLO. Section 3 presents our numerical results for the differential rate and the moments in the on-shell scheme and the kinetic scheme. We will discuss also the impact on the decay $B \rightarrow X_c \tau \bar{\nu}_\tau$. We conclude in Section 4.

2 Details of the calculation

Let us now discuss the details of the calculation. We consider the semileptonic decay of a bottom quark mediated by the weak interaction

$$b(p_b) \rightarrow X_c(p_X) \ell(p_\ell) \bar{\nu}_\ell(p_\nu), \quad \text{with } \ell = e, \mu, \tau, \quad (1)$$

where X_c generically denotes a state containing a charm quark, plus additional gluons and/or quarks. The mass of the charged lepton ℓ is denoted by m_ℓ while the neutrino is considered massless. The masses of the bottom and charm quark are m_b and m_c , respectively, and we introduce their ratio $\rho = m_c/m_b$. In the following we study the spectrum of the leptonic invariant mass $q^2 = p_L^2$ with $p_L = p_\ell + p_\nu$. We begin by writing the differential rate w.r.t. q^2 as

$$\frac{d\Gamma}{d\hat{q}^2} = \frac{G_F^2 m_b^5}{192\pi^3} |V_{cb}|^2 \left[F_0(\rho, \hat{q}^2) + \frac{\alpha_s}{\pi} F_1(\rho, \hat{q}^2) + \left(\frac{\alpha_s}{\pi}\right)^2 F_2(\rho, \hat{q}^2) \right] + \mathcal{O}\left(\frac{1}{m_b^2}\right), \quad (2)$$

where $\hat{q}^2 = q^2/m_b^2$ and F_i stands for the differential decay rate at leading, next-to-leading and next-to-next-to-leading order, respectively. The functions F_0 and F_1 are known since

¹We contacted the authors of Ref. [29], however they could not retrieve their original Monte Carlo code.

a long time [21]. For the power corrections up to $1/m_b^3$ the NLO corrections have been presented in Refs. [27, 37, 38]. The quark masses m_b and m_c are renormalized in the on-shell scheme. The strong coupling constant $\alpha_s = \alpha_s^{(5)}(\mu_s)$ is renormalized in the $\overline{\text{MS}}$ scheme with five active flavours with μ_s being the renormalization scale.

In order to calculate the NNLO QCD corrections to the q^2 spectrum, we follow the method of Refs. [27, 37]. The idea is to consider the differential rate in the presence of a constraint on q^2 . The phase-space decomposition suitable for $b \rightarrow X_c \ell \bar{\nu}_\ell$ is carried out by assuming a sequence of two two-body decays. First, the bottom quark decays into an off-shell W -boson and the charm quark, then the virtual W -boson decays into the lepton and the neutrino:

$$d\Gamma = \frac{(2\pi)^d}{2m_b} \delta(p_L^2 - q^2) W_{\mu\nu} L^{\mu\nu} d\Phi_2(p_b; p_L, p_X) d\Phi_2(p_L; p_\ell, p_\nu) (2\pi)^{d-1} dq^2 \quad (3)$$

where the integration is performed in a d -dimensional space, with $d = 4 - 2\epsilon$. $W^{\mu\nu}$ and $L^{\mu\nu}$ are the hadronic and leptonic tensors. The element of n -body phase space is given by

$$d\Phi_n(P; p_1, \dots, p_n) = \delta^{(d)}\left(P - \sum_{i=1}^n p_i\right) \prod_{i=1}^n \frac{d^{d-1}p_i}{(2\pi)^{d-1} 2E_i}. \quad (4)$$

The constraint $\delta(p_L^2 - q^2)$ enforces the dilepton system to have an invariant mass equal to q^2 . Since the hadronic tensor depends only on p_L and p_b , we can integrate the leptonic tensor with respect to the phase-space of charged lepton and neutrino [38]:

$$\begin{aligned} \mathcal{L}^{\mu\nu}(p_L) &= \int L^{\mu\nu} d\Phi_2(p_L; p_e, p_\nu) \\ &= \frac{1}{384\pi^5} \left(1 - \frac{m_\ell^2}{p_L^2}\right)^2 \left[\left(1 + \frac{2m_\ell^2}{p_L^2}\right) p_L^\mu p_L^\nu - g^{\mu\nu} p_L^2 \left(1 + \frac{m_\ell^2}{2p_L^2}\right) \right] + \mathcal{O}(\epsilon). \end{aligned} \quad (5)$$

Higher order terms in ϵ are not necessary since the leptonic tensor does not enter into the renormalization, i.e. $\mathcal{L}^{\mu\nu}$ is always contracted with the renormalized hadronic tensor. After inserting Eq. (5) into the differential rate formula, we represent the δ function as the imaginary part of a propagator:

$$\delta(p_L^2 - q^2) \rightarrow \frac{1}{2\pi i} \left[\frac{1}{p_L^2 - q^2 - i0} - \frac{1}{p_L^2 - q^2 + i0} \right], \quad (6)$$

In other words, we treat $\delta(p_L^2 - q^2)$ as an on-shell condition for a “fake” particle. Next we apply the reverse unitarity method [39] and map the calculation of the various interference terms integrated over the final state phase-space into the evaluation of “cuts” of forward $b \rightarrow b$ scattering amplitudes. In this way, the differential rate can be obtained from the imaginary part of a $b \rightarrow b$ two-point amplitude, where the two leptons with constrained invariant mass are replaced by a fake (colorless) spin-1 particle with mass equal to q^2 (see Fig. 1). Note that with this method, we need to consider loop diagrams with one loop

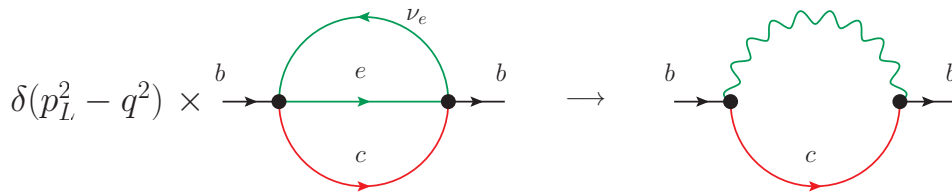


Figure 1: Phase space intergration in the presence of the constraint on the leptonic invariant mass $\delta(p_L^2 - q^2)$ is mapped into the cuts of forward $b \rightarrow b$ scattering amplitude where the two leptons are replaced by a fake spin-1 massive particle.

less compared to the original diagrams, i.e. to calculate the q^2 spectrum at LO, NLO and NNLO we have to consider one-, two- and three-loop diagrams. On the other hand, the Feynman integrals now depend on two dimensionless variables: ρ and \hat{q}^2 .

Let us now discuss the technical details of the calculation. We generate with `qgraf` [40] one, two and three loop diagrams (as the ones on the r.h.s. of Fig. 1) and use `Tapir` [41] to map each diagram to a predefined integral family. We use the program `exp` [42] to rewrite the output to `FORM` [43] notation. In this way we express the three-loop $b \rightarrow b$ amplitude as linear combinations of scalar Feynman integrals with nine indices, where eight correspond to the exponents of propagators and the remaining one to the exponent of an irreducible numerator. In total we have 21 integral families at three loops.

Before performing the IBP reduction, we find with a basis of master integrals such that the denominators in the reduction tables completely factorize into polynomials depending either on ρ and \hat{q}^2 or d (see Ref. [44, 45]). To construct this basis, we first reduce a set of seed integrals up to two dots and one scalar product for every integral family individually with the help of `Kira` [46, 47] and `Fermat` [48]. As initial basis we simply take the default master integrals. These reduction tables then serve as input to search for a good basis for every family with the help `ImproveMasters.m` developed in Ref. [44].

The IBP reduction of the integrals appearing in the amplitude is then performed with `Kira`. First, we reduce the integrals for every family individually to the good basis of this family. Then we employ symmetries between the families to reduce the number of master integrals. Afterwards we identify the master integrals which have an imaginary part while setting to zero those which are purely real, e.g. tadpole integrals. We find one, six and 98 master integrals at one, two and three loops.

We solve the master integrals in an analytic way by using the method of differential equations [49, 50]. We establish a set of differential equations by differentiating the 98 master integrals with respect to ρ and \hat{q}^2 and reducing the resulting integrals again to master integrals with `Kira`. We obtain a system of the form

$$\frac{\partial \mathbf{J}}{\partial \rho} = \mathbb{M}_\rho(\rho, \hat{q}^2, \epsilon) \mathbf{J}, \quad \frac{\partial \mathbf{J}}{\partial \hat{q}^2} = \mathbb{M}_{q^2}(\rho, \hat{q}^2, \epsilon) \mathbf{J}, \quad (7)$$

where $\mathbf{J} = (J_1, \dots, J_{98})$ is the set of master integrals, ϵ is the dimensional regularization parameter while \mathbb{M}_ρ and \mathbb{M}_{q^2} are 98×98 matrices, rational in ρ , \hat{q}^2 and ϵ .

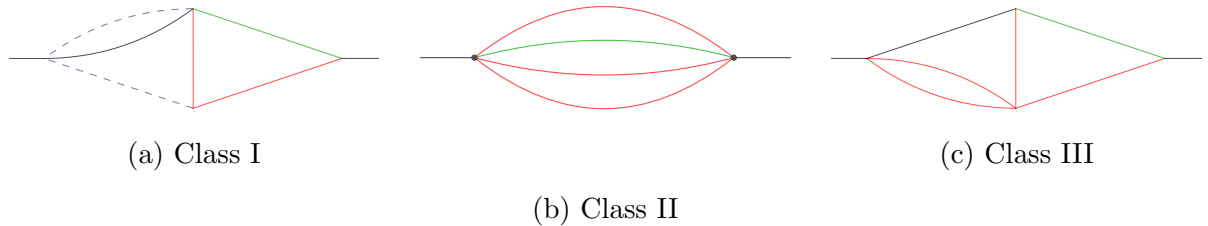


Figure 2: Sample of master integrals. Black, red and green lines denoted massive propagators with mass equal to m_b , m_c and $\sqrt{q^2}$. Dashed lines are massless propagators. The master integrals can have cuts through only one charm propagator (a), only three charm propagators (b) and both kind of cuts (c).

For the decay rate, we need only the imaginary parts of the master integrals, i.e. the sum of all possible cuts. Before discussing their solution, it is useful to divide them into three classes according to their cuts:

- (i) master integrals with cuts only through one charm quark propagator (and the fake particle with mass q^2). A sample integral is shown in Fig. 2a.
- (ii) integrals where the cuts go through three charm propagators (see Fig. 2b).
- (iii) integrals with both kind of cuts, i.e. one and three charm cuts (see Fig. 2c).

We would like to bring the system of differential equations in canonical form (or ϵ -form) [51] and express the master integrals in terms of GPLs. Class II contains integrals beyond GPLs such as the sunrise diagram in Fig. 2b with two unequal masses.

However, as observed already for the analytic calculation of the total rate at NNLO presented in Ref. [52], the contribution given by cuts through three charm quarks can be neglected for realistic values of the ratio m_c/m_b . It corresponds to the decay channel $b \rightarrow c\bar{c}cl\bar{\nu}_\ell$, which is rare and present only if $0 < \rho < 1/3$. For $m_c/m_b \simeq 0.25$, the branching ratio is very small, $O(10^{-7})$, because of the phase-space suppression and totally negligible compared to the current experimental accuracy.

Our strategy therefore is to solve the differential equations by considering only the cuts with one charm quark and neglecting the cuts with three charm quarks. To this end, we can effectively remove the masters in class II, while for class III we pick up only the one-charm cut contributions in the boundary conditions.

After such simplifications, the number of master integrals reduces to 87 and we proceed to find a basis transformation $\mathbb{T}(\rho, \hat{q}^2, \epsilon)$ such that the masters in the new basis $\mathbf{J} = \mathbb{T}\tilde{\mathbf{J}}$ satisfy a set of differential equations in canonical form. We change variables from ρ and \hat{q}^2 to

$$x_{\pm} = \frac{1}{2} (1 - \hat{q}^2 + \rho^2 \pm \lambda^{1/2}(1, \hat{q}^2, \rho^2)), \quad (8)$$

with $0 \leq x_- \leq x_+ \leq 1$ and $\lambda(a, b, c) = a^2 + b^2 + c^2 - 2ab - 2ac - 2bc$. To find a rational transformation \mathbb{T} , we use `Libra` [53], which implements the Lee's algorithm [54], in

combination with `Fermatica` [55] to speed up the matrix transformations via the interface to the CAS program `FerMat`.

As a first step, we find suitable transformations acting on the diagonal blocks that put them into ϵ -form. At NLO, we observe that it is possible to bring the system of differential equations in canonical form when written in terms of the variables x_{\pm} , however at NNLO this is not possible anymore. The eigenvalues of the residue matrices of some blocks are of the form $a\epsilon \pm 1/2$, with a an integer number. Balanced transformations can only raise or lower the eigenvalues by an integer, so in order to bring such blocks into ϵ -form, we need to apply an additional variable change. We find that all such eigenvalues with half-integers can be removed by switching from x_+ and x_- to the variables u and v defined by

$$\rho = v, \quad \hat{q}^2 = (1 - uv) \left(1 - \frac{v}{u}\right), \quad (9)$$

with $0 < v \leq u \leq 1$. However, we find it convenient not to perform the variable transformation globally because this would increase the degree of the poles in the residue matrices, making the reduction to ϵ -form computationally more challenging. Instead we take advantage of the `Notations` mechanism implemented in `Libra`. The idea is to work with a system still expressed in terms of x_+ and x_- , but with the introduction of the notation

$$u^2 = \frac{x_-}{x_+}. \quad (10)$$

In each subblock, all variables x_+ , x_- and u appear. However the dependence of the latter on x_+ and x_- is always taken into account when computing derivatives and it is automatically simplified to first-order polynomial in u . After bringing all diagonal blocks to ϵ -form, `Libra` automatically reduces the off-diagonal blocks to Fuchsian form and finds a suitable transformation independent of x_+ and x_- to factorize out ϵ . In the end, we bring the system of differential equation in canonical form:

$$d\tilde{\mathbf{J}}(u, v, \epsilon) = \epsilon d\mathbb{A}(u, v) \tilde{\mathbf{J}}(u, v, \epsilon), \quad (11)$$

where

$$\mathbb{A}(u, v) = \sum_{i=1}^{14} A_i \log(\alpha_i). \quad (12)$$

A_i are 87×87 matrices with rational numbers and α_i are the letters

$$\begin{aligned} \alpha_1 &= 1 - u, & \alpha_2 &= u, & \alpha_3 &= 1 + u, \\ \alpha_4 &= 1 - v, & \alpha_5 &= v, & \alpha_6 &= 1 + v, \\ \alpha_7 &= u - v, & \alpha_8 &= u + v, & \alpha_9 &= 1 - uv, \\ \alpha_{10} &= 1 + u^2 - 2uv, & \alpha_{11} &= 1 + u^2 - uv, & \alpha_{12} &= 1 + uv, \\ \alpha_{13} &= u - v - u^2v, & \alpha_{14} &= 2u - v - u^2v. \end{aligned} \quad (13)$$

Since all letters are linear in v , we write the solution of the differential equation in terms of GPLs in v and letters that might depend on u , as well as Harmonic polylogarithms in u .

The boundary conditions to the differential equations are obtained using the auxiliary mass flow method [56, 57] as implemented in `AMFlow` [58]. We compute all 87 master integrals in four different kinematic points:

$$(q^2/m_b^2, m_c^2/m_b^2) \in \{(1/5, 1/5), (4/25, 4/25), (1/32, 1/16), (1/16, 1/32)\} . \quad (14)$$

These points are sufficient to fix all boundary constants and at least have two additional kinematic points to check the resulting integrals.² The master integrals are computed with sufficient numerical precision in order to obtain the boundary constants of the differential equations written in terms of transcendental numbers using the `PSLQ` algorithm [59].

3 Results

After the evaluation of the master integrals (one-charm cuts), we insert them into the amplitude and perform the wave function and mass renormalization in the on-shell scheme [60–64], while we use $\overline{\text{MS}}$ for the strong coupling constant.

Our main results are the analytic expressions for the functions F_0, F_1 and F_2 in the differential decay rate in Eq. (2). They are written in terms of GPLs depending on u and v , as defined in Eq. (9), which can be evaluated numerically to high accuracy, e.g. with `GiNaC` [65] and `PolyLogTools` [66]. The explicit expressions for F_0, F_1 and F_2 are given as ancillary files [67].

Moments of the q^2 spectrum are defined by

$$Q_n(q_{\text{cut}}^2) = \frac{1}{\Gamma_0} \int_{q^2 > q_{\text{cut}}^2} (q^2)^n \frac{d\Gamma}{dq^2} dq^2, \quad (15)$$

where $\Gamma_0 = G_F^2 m_b^5 |V_{cb}|^2 / (192\pi^3)$. The moments can be expressed as series expansions in α_s :

$$Q_n = \sum_{i \geq 0} Q_n^{(i)} \left(\frac{\alpha_s(\mu_s)}{\pi} \right)^i . \quad (16)$$

From the expressions for F_i , we calculate the coefficients in the perturbative expansion via one-dimensional numerical integrations of the functions F_i :

$$\begin{aligned} \frac{Q_n^{(i)}(q_{\text{cut}}^2)}{m_b^{2n}} &= \int_{\hat{q}^2 > \hat{q}_{\text{cut}}^2} (\hat{q}^2)^n F_i(\rho, \hat{q}^2) d\hat{q}^2 \\ &= \int_{u_{\text{min}}}^1 \left[(1 - u\rho) \left(1 - \frac{\rho}{u} \right) \right]^n \frac{(1 - u^2)\rho}{u^2} F(\rho, \hat{q}^2(\rho, u)) du, \end{aligned} \quad (17)$$

²Aside from integrals in class III, here the last two points allow for the three-charm cut and thus are not used.

where

$$u_{\min} = \frac{1}{2\rho} [1 - \hat{q}_{\text{cut}}^2 + \rho^2 - \lambda^{1/2}(1, \hat{q}_{\text{cut}}^2, \rho^2)], \quad (18)$$

which reduces to $u_{\min} = \rho$ for $\hat{q}_{\text{cut}}^2 = 0$. We also define the normalized q^2 moments as

$$\langle (q^2)^n \rangle_{q^2 \geq q_{\text{cut}}^2} = \frac{Q_n(q_{\text{cut}}^2)}{Q_0(q_{\text{cut}}^2)}, \quad (19)$$

and the centralized moments as

$$q_1(q_{\text{cut}}^2) = \langle q^2 \rangle_{q^2 \geq q_{\text{cut}}^2}, \quad q_n(q_{\text{cut}}^2) = \left\langle (q^2 - \langle q^2 \rangle)^n \right\rangle_{q^2 \geq q_{\text{cut}}^2} \quad \text{for } n \geq 2. \quad (20)$$

Moreover, with \hat{q}_n we denote $\hat{q}_n = q_n/m_b^{2n}$.

On-shell scheme

We now present our results for the centralized moments in the on-shell scheme. We set the quark masses to $m_b^{\text{OS}} = 4.6$ GeV and $m_c^{\text{OS}} = 1.15$ GeV and numerically evaluate the coefficients in the perturbative expansions for Q_n , with $n = 1, \dots, 4$. Afterwards, we reexpand the ratios in Eqs. (19) and (20) in α_s up to second order. Our results for the moments without cuts ($q_{\text{cut}}^2 = 0$ GeV²) read

$$\begin{aligned} \hat{q}_1 &= 0.2185 \left[1 + 0.1276 \left(\frac{\alpha}{\pi} \right) + 0.4460 \left(\frac{\alpha}{\pi} \right)^2 \right], \\ \hat{q}_2 &= 0.02040 \left[1 + 0.1382 \left(\frac{\alpha}{\pi} \right) + 0.9197 \left(\frac{\alpha}{\pi} \right)^2 \right], \\ \hat{q}_3 &= 1.1042 \times 10^{-3} \left[1 - 0.2271 \left(\frac{\alpha}{\pi} \right) + 1.097 \left(\frac{\alpha}{\pi} \right)^2 \right], \\ \hat{q}_4 &= 8.895 \times 10^{-4} \left[1 + 0.1677 \left(\frac{\alpha}{\pi} \right) + 1.591 \left(\frac{\alpha}{\pi} \right)^2 \right], \end{aligned} \quad (21)$$

which are in good agreement with the NNLO results presented in Ref. [34]. For a cut of $q_{\text{cut}}^2 = 3$ GeV², we obtain

$$\begin{aligned} \hat{q}_1 &= 0.3022 \left[1 + 0.06894 \left(\frac{\alpha}{\pi} \right) + 0.3428 \left(\frac{\alpha}{\pi} \right)^2 \right], \\ \hat{q}_2 &= 0.01151 \left[1 + 0.1433 \left(\frac{\alpha}{\pi} \right) + 1.209 \left(\frac{\alpha}{\pi} \right)^2 \right], \\ \hat{q}_3 &= 5.1013 \times 10^{-4} \left[1 - 0.2171 \left(\frac{\alpha}{\pi} \right) + 0.5447 \left(\frac{\alpha}{\pi} \right)^2 \right], \\ \hat{q}_4 &= 2.857 \times 10^{-4} \left[1 + 0.1634 \left(\frac{\alpha}{\pi} \right) + 1.849 \left(\frac{\alpha}{\pi} \right)^2 \right]. \end{aligned} \quad (22)$$

Kinetic scheme

We discuss now the impact of higher-order QCD corrections to q^2 moments once a short-distance mass scheme is adopted for the quark masses. We concentrate on the kinetic scheme employed in the global fits of Refs. [8–10, 17, 68]. In this scheme the on-shell mass of the bottom quark is replaced by the kinetic mass [64, 69–71] via the relation

$$m_b^{\text{kin}}(\mu) = m_b^{\text{OS}} - [\overline{\Lambda}(\mu)]_{\text{pert}} - \frac{[\mu_\pi^2(\mu)]_{\text{pert}}}{2m_b^{\text{kin}}(\mu)} - O\left(\frac{1}{(m_b^{\text{kin}})^2}\right), \quad (23)$$

while the charm quark mass is converted to the $\overline{\text{MS}}$ scheme. At the same time, we include the contribution from power corrections to the moments up to $1/m_b^3$ (the relevant expressions can be retrieved from [15, 27]). In the kinetic scheme, we redefine the HQE parameters μ_π^2 and ρ_D^3 in the following way:

$$\mu_\pi^2(0) = \mu_\pi^2(\mu) - [\mu_\pi^2(\mu)]_{\text{pert}}, \quad \rho_D^3(0) = \rho_D^3(\mu) - [\rho_D^3(\mu)]_{\text{pert}}. \quad (24)$$

Note that μ_π^2 drops out for centralized q^2 moments, leaving a dependence only on ρ_D^3 . The perturbative version of μ_π^2 and ρ_D^3 up to $\mathcal{O}(\alpha_s^3)$ can be found in the Appendix of Ref. [64]. The Wilsonian cutoff μ plays the role of scale separation between the short- and long-distance regimes in QCD.

In order to present our benchmark predictions of the q^2 moments for validation and comparison, we report the series expansion for centralized moments with $q_{\text{cut}}^2 = 0 \text{ GeV}^2$ and $q_{\text{cut}}^2 = 4 \text{ GeV}^2$. We adopt the HQE parameter definitions employed in Refs. [8, 9, 72] (the so-called *perp* basis). We use scheme (A) as defined in Ref. [34]: in a first step the expressions for centralized moments are obtained in the on-shell scheme where we retain terms up to $O(\alpha_s^2)$ at partonic level ($1/m_b^0$) while we discard higher QCD corrections for the subleading power corrections. Afterwards we apply the transition to the kinetic scheme.

We set the renormalization scale of the strong coupling constant $\mu_s = m_b^{\text{kin}}$ and use $\alpha_s^{(4)}(m_b^{\text{kin}})$ as expansion parameter, i.e. we decouple the bottom quark from the running of α_s , and we reexpand the leading $1/m_b$ term in $\alpha_s^{(4)}$ up to second order. We use the input values

$$\begin{aligned} m_b^{\text{kin}}(1 \text{ GeV}) &= 4.526 \text{ GeV}, & \overline{m}_c(3 \text{ GeV}) &= 0.989 \text{ GeV}, \\ \mu &= 1 \text{ GeV}, & \alpha_s^{(4)}(m_b^{\text{kin}}) &= 0.2186. \end{aligned} \quad (25)$$

In the following we present the results for the various contribution at leading order in the $1/m_b$ expansion for two different values of q_{cut}^2 . We do not report the contribution from power suppressed terms, however the terms originating from $[\rho_D^2(\mu)]_{\text{pert}}$ are included. Our results for the moments for $q_{\text{cut}}^2 = 0 \text{ GeV}^2$ read

$$\begin{aligned} \hat{q}_1 &= 0.2329 \left[1 - 0.1524 \left(\frac{\alpha_s}{\pi}\right) - 1.791 \left(\frac{\alpha_s}{\pi}\right)^2 \right], \\ \hat{q}_2^2 &= 0.02353 \left[1 - 0.516 \left(\frac{\alpha_s}{\pi}\right) - 4.474 \left(\frac{\alpha_s}{\pi}\right)^2 \right], \end{aligned}$$

$$\begin{aligned}
\hat{q}_3 &= 0.001451 \left[1 - 1.007 \left(\frac{\alpha_s}{\pi} \right) - 7.408 \left(\frac{\alpha_s}{\pi} \right)^2 \right], \\
\hat{q}_4 &= 0.001202 \left[1 - 0.8404 \left(\frac{\alpha_s}{\pi} \right) - 8.724 \left(\frac{\alpha_s}{\pi} \right)^2 \right].
\end{aligned} \tag{26}$$

In case we apply a cut of $q_{\text{cut}}^2 = 4 \text{ GeV}^2$ we obtain

$$\begin{aligned}
\hat{q}_1 &= 0.3503 \left[1 - 0.1628 \left(\frac{\alpha_s}{\pi} \right) - 1.437 \left(\frac{\alpha_s}{\pi} \right)^2 \right], \\
\hat{q}_2 &= 0.01102 \left[1 - 0.7408 \left(\frac{\alpha_s}{\pi} \right) - 6.236 \left(\frac{\alpha_s}{\pi} \right)^2 \right], \\
\hat{q}_3 &= 0.0005113 \left[1 + 0.06583 \left(\frac{\alpha_s}{\pi} \right) + 4.269 \left(\frac{\alpha_s}{\pi} \right)^2 \right], \\
\hat{q}_4 &= 0.0002659 \left[1 - 0.5384 \left(\frac{\alpha_s}{\pi} \right) - 11.69 \left(\frac{\alpha_s}{\pi} \right)^2 \right].
\end{aligned} \tag{27}$$

We performed a comparison also with the corrections of order $\alpha_s^2\beta_0$ (the so-called BLM corrections [73]) recently presented in Table 1 of Ref. [10] and found good agreement. From the knowledge of the complete NNLO corrections, we observe that in the kinetic scheme the non-BLM contribution to the moments at $\mathcal{O}(\alpha_s^2)$ has in general the opposite sign of the BLM contribution, and is of comparable size. We conclude that the BLM approximation tends to overestimate the NNLO corrections, especially in case one uses $\bar{m}_c(3 \text{ GeV})$ as reference mass for the charm quark.

Let us now discuss the size of the NNLO corrections and the impact on the global fits for V_{cb} . In Figures 3 and 4 we show our results for the first four centralized moments as a function of q_{cut}^2 . The predictions are compared with the Belle and Belle II measurements [18, 19]. At variance with the numerical values given in Eqs. 26 and 27, in the plots we adopt the *RPI* basis from Refs. [15, 16] and the values from the fit in Ref. [17] for the HQE parameters, m_b and m_c .

The green curves correspond to the LO prediction with power corrections up to $1/m_b^3$. The blue curves include QCD NLO correction up to $1/m_b^3$, where we also include the α_s corrections to μ_G^2 and ρ_D^3 calculated in Ref. [27]. The red curves, compared to the blue ones, additionally include the NNLO corrections at leading order in $1/m_b$ calculated in this article, which are denoted by NNLO' in the plots. The error bands are obtained by varying the renormalization scale in the range $m_b^{\text{kin}}/2 < \mu_s < 2m_b^{\text{kin}}$ and choosing $\mu_s = m_b^{\text{kin}}$ as reference scale for the central value. We do not show the parametric uncertainty stemming from the HQE parameters. The lower panel in each plot shows the ratio between the prediction at NNLO and NLO.

In Figure 3, we show the moments obtained with charm mass at a scale of 2 GeV, which is the default choice in the fit in Ref. [17]. We observe that the NNLO corrections shift the prediction for q_1 and q_2 by a few percent in the low q_{cut}^2 range. For the third and fourth moment the impact is larger and close to a 10-15% effects. The relative contribution at

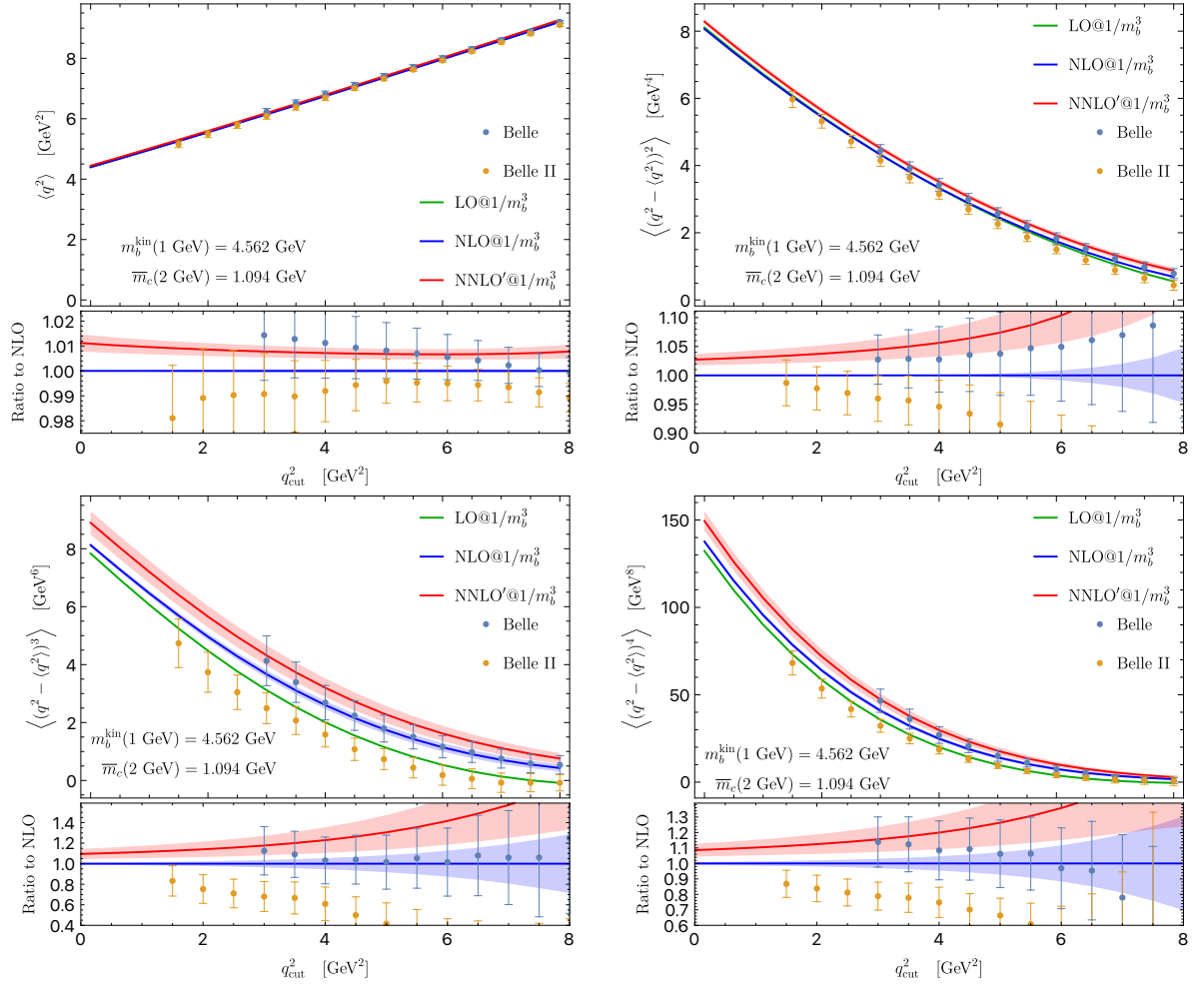


Figure 3: The first four q^2 moments of $B \rightarrow X_c \ell \bar{\nu}_\ell$ as a function of the lower cut q_{cut}^2 . The heavy quark masses are $m_b^{\text{kin}}(1 \text{ GeV}) = 4.562 \text{ GeV}$ and $\bar{m}_c(2 \text{ GeV}) = 1.094 \text{ GeV}$. For the HQE parameter we adopt the RPI basis up to $1/m_b^3$ [15, 16] and values from the fit in Ref. [17]. Measurements from Belle [18] and Belle II [19].

higher values of q_{cut}^2 becomes larger since the LO central value tends to vanish close to the end point. Note that the use of $\bar{m}_c(2 \text{ GeV})$ leads to accidentally small corrections at $O(\alpha_s)$ for all the moments. For q_1 and q_2 one can observe the overlap between the blue and green bands, while the red lines are much more separated. Consequently, scale-variation alone does not provide a reliable uncertainty estimate for the NLO prediction. In fact in this approximation, the scale uncertainty comes only from the variation of α_s . Since α_s is multiplied by a small number in case one uses $\bar{m}_c(2 \text{ GeV})$, a rather small uncertainty is obtained. Improving the prediction from the NLO to the NNLO, we observe that the $O(\alpha_s^2)$ coefficient is not suppressed anymore and therefore NNLO error bands become larger than the NLO ones.

A better behaviour of the perturbative series is observed utilizing instead $\bar{m}_c(3 \text{ GeV}) =$

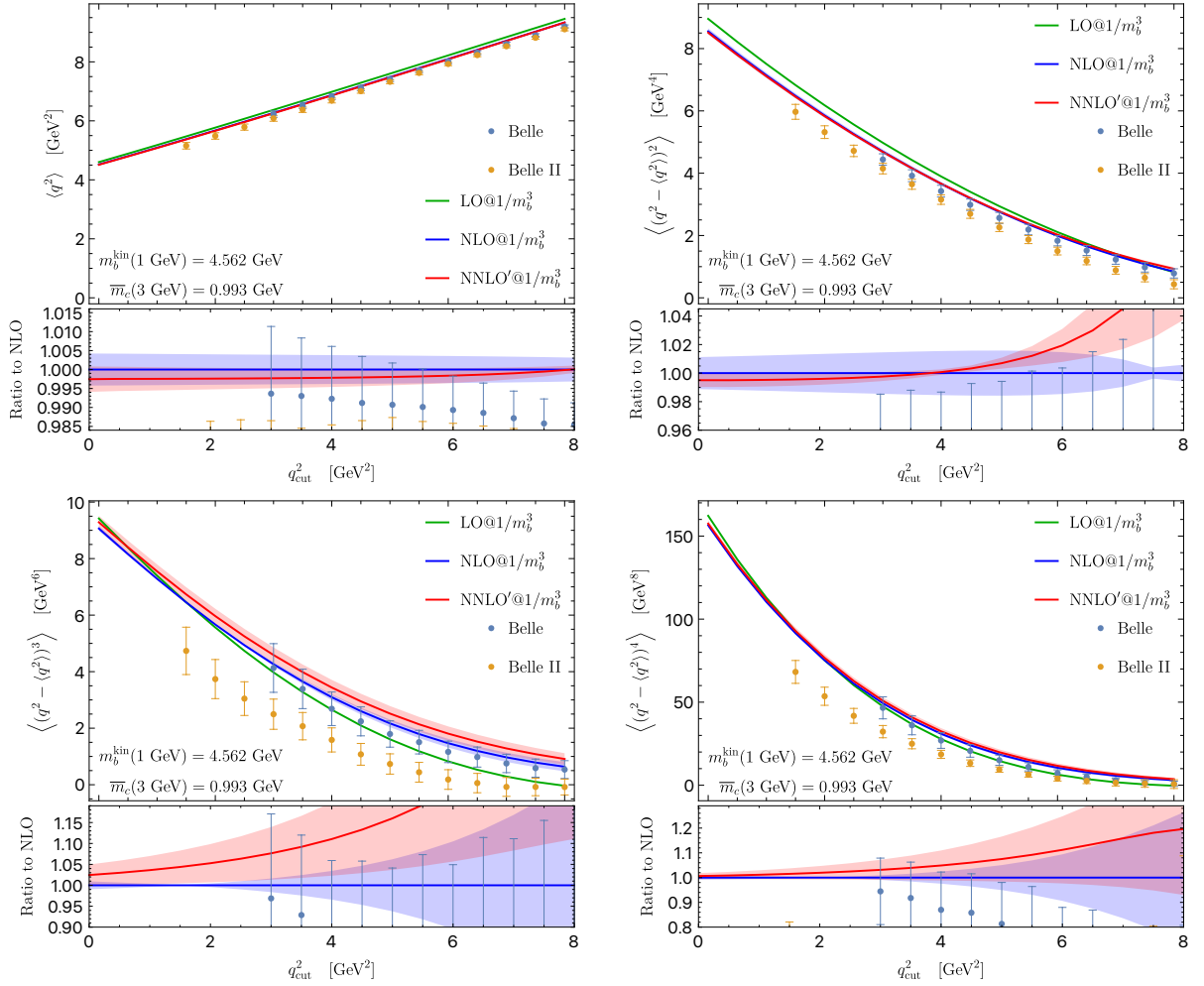


Figure 4: The first four q^2 moments of $B \rightarrow X_c \ell \bar{\nu}_\ell$ as a function of the lower cut q_{cut}^2 . The heavy quark masses are $m_b^{\text{kin}}(1 \text{ GeV}) = 4.562 \text{ GeV}$ and $\bar{m}_c(3 \text{ GeV}) = 0.993 \text{ GeV}$. For the HQE parameter we adopt the RPI basis up to $1/m_b^3$ [15,16] and values from the fit in Ref. [17]. Measurements from Belle [18] and Belle II [19].

0.993 GeV. The results are presented in Figure 4. Notice that now the $O(\alpha_s^2)$ corrections are smaller than the $O(\alpha_s)$ ones, indicating a much better behaved expansion. For the first and second moment the scale uncertainty is reduced from NLO to NNLO and the error bands overlap. Even though the error bands overlap for the third and fourth moment, we still observe a larger uncertainty at NNLO. This can be explained by the fact that the third and fourth moments, especially at high values of q_{cut}^2 , receive sizable contributions from the power suppressed terms, which include perturbative corrections only up to NLO. The uncertainty is not reduced in this case because cancellation of the μ_s dependence at partonic level is spoiled by the lower accuracy in the perturbative expansion of the $1/m_b^2$ and $1/m_b^3$ terms.

Another notable effect observed in Fig. 3 is that after inclusion of the NNLO corrections

the curves move to values higher than the experimental data points. This does not indicate a tension between data and theory. In fact, since we use the HQE parameters from a fit accurate only up to NLO at partonic level [17], we naturally expect the NLO curves to show better agreement with the data. Notice that the blue curves include also the NLO corrections at $1/m_b^2$ and $1/m_b^3$, which was not the case in Ref. [17]. The major effect in global fits after including the NNLO corrections would be a change of the favoured values of the HQE parameters in order to shift downwards the red curves and accommodate the predictions with the data. In particular, since ρ_D has a major impact in the q^2 moments and enters with negative coefficients, a fit with NNLO corrections would prefer higher values for ρ_D compared to Ref. [17].

In addition to the analysis of the moments in the *RPI* basis, we analyzed also the prediction with the fit setup from Ref. [10] and using the *perp* basis for defining the HQE parameters. We reached similar conclusions for what concerns the use of a charm mass at a scale of 2 GeV or 3 GeV: a charm mass at 3 GeV yields a better behaviour of the perturbative series while a 2 GeV charm mass underestimates uncertainties at NLO. For completeness, we report in Fig. 5 our results for a charm mass $\overline{m}_c(2 \text{ GeV}) = 1.092 \text{ GeV}$, the default scheme in Ref. [10]. We also mention that since the $\alpha_s^2\beta_0$ corrections overestimates the α_s^2 corrections, the NNLO predictions shown by the red curves in Fig. 5 lie below the experimental data. A curve showing the q^2 moment prediction with only the $\alpha_s^2\beta_0$ corrections would appear above the red curves, more in agreement with data. We conclude that the inclusion of the complete NNLO corrections in the fit of [10] would bring the red curves upwards, towards the experimental data, preferring a lower value for ρ_D (also in the *perp* basis the coefficient of ρ_D is negative).

Decay into a massive tau lepton

While the $\mathcal{O}(\alpha_s^2)$ contributions to the q^2 spectrum are most relevant for the decay into light leptons, our expressions also apply to inclusive $b \rightarrow X_c \tau \bar{\nu}_\tau$ decays. The first measurement of the ratio

$$R(X) = \frac{\Gamma_{B \rightarrow X \tau \bar{\nu}_\tau}}{\Gamma_{B \rightarrow X \ell \bar{\nu}_\ell}} \quad (28)$$

was recently performed by the Belle II experiment [74]. The current level of experimental precision is severely limited by systematic uncertainties related to the modelling of $B \rightarrow X \tau / \ell \bar{\nu}_\tau / \ell$ decays. However, recent progress in the description of B meson decays into excited charm meson states [75] will allow to address this issue in a data-driven way in the future, making the inclusion of $\mathcal{O}(\alpha_s^2)$ corrections relevant.

In the on-shell scheme, our results for the integrated $b \rightarrow X_c \tau \bar{\nu}_\tau$ decay rate without cut on q^2 agrees with Ref. [29]. In the kinetic scheme, with $m_b^{\text{kin}}(1 \text{ GeV}) = 4.526 \text{ GeV}$, $\overline{m}_c(3 \text{ GeV}) = 0.993 \text{ GeV}$ and at leading order in $1/m_b$, we obtain

$$R(X_c) = 0.241 \left[1 - 0.156 \left(\frac{\alpha_s}{\pi} \right) - 1.766 \left(\frac{\alpha_s}{\pi} \right)^2 \right]. \quad (29)$$

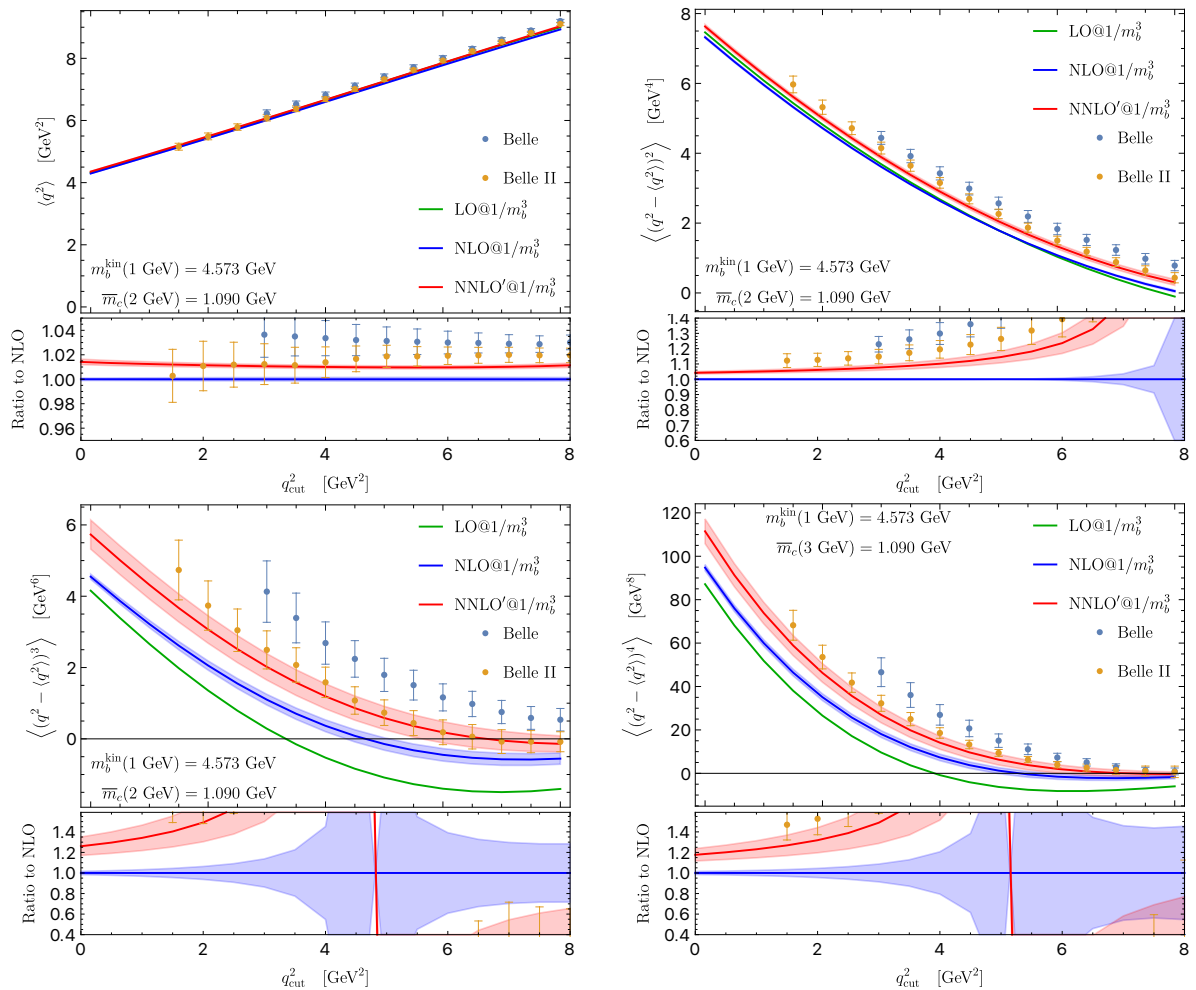


Figure 5: The first four q^2 moments of $B \rightarrow X_c \ell \bar{\nu}_\ell$ as a function of the lower cut q^2_{cut} . The heavy quark masses are $m_b^{\text{kin}}(1 \text{ GeV}) = 4.573 \text{ GeV}$ and $\bar{m}_c(2 \text{ GeV}) = 1.092 \text{ GeV}$. For the HQE parameter we adopt the perp basis up to $1/m_b^3$ [72] and values from the fit in Ref. [10]. The central values are obtained for a renormalization scale $\mu_s = m_b^{\text{kin}}/2$. Measurements from Belle [18] and Belle II [19].

The perturbative convergence is similar to the case of the q^2 moments. This prediction can be improved by incorporating $1/m_b$ suppressed terms at LO and NLO [38].

Our results allow to obtain predictions for $R(X_c)$ with a lower cut on q^2 . For $q^2_{\text{cut}} = 6 \text{ GeV}^2$, we obtain

$$R(X_c) \Big|_{q^2 > 6 \text{ GeV}^2} = 0.350 \left[1 - 0.782 \left(\frac{\alpha_s}{\pi} \right) - 8.355 \left(\frac{\alpha_s}{\pi} \right)^2 \right]. \quad (30)$$

The higher order corrections clearly become more relevant if a cut is introduced.

Furthermore, the ratio increases with increasing q^2_{cut} , as terms proportional to m_τ^2/q^2 and phase-space effects become less relevant. Consequently, it could be advantageous to

perform measurements of $R(X)$ using a lower cut on q^2 in the future, as it enriches the fraction of $B \rightarrow X\tau\bar{\nu}_\tau$ decays, rejects backgrounds and cuts away the regions where the $B \rightarrow X\ell\nu$ modelling is most problematic. In addition a lower cut on q^2 allows for the improved inclusion of momentum requirements on signal leptons due to detector thresholds and the reduction of uncertainties associated to the modelling of final state radiation [76]. Most of the analysis strategy of the Belle measurement of the q^2 moments [18] could thus carry over to a future measurement of $R(X)$, with the exception of a cut on the difference of the missing energy and the missing momentum in a given event.³

4 Conclusions

In this article we presented the complete NNLO QCD corrections to the q^2 spectrum of inclusive semileptonic B decays. The differential rate with respect to the leptonic invariant mass q^2 is obtained by calculating the imaginary part of the $b \rightarrow b$ 2-point function in the presence of a constraint on q^2 , which can be implemented in a convenient way by replacing the charged lepton-neutrino loop with a fake particle with mass q^2 . After reduction to master integrals, we leverage the method of differential equations to calculate the decay rate analytically. To this end, we restricted the calculation to the cuts through only one charm line which allowed us to bring the system of differential equations in canonical form and express the master integrals in terms of GPLs.

In light of the recent measurements of Belle and Belle II of the q^2 moments, we studied the impact of the NNLO corrections on the moments as a function of q_{cut}^2 . We observe that the $\mathcal{O}(\alpha_s^2)$ corrections are sizable especially for the default choice of the charm mass $\bar{m}_c(2\text{ GeV})$ in the global fits of [10, 17]. The relative ratio to the NLO prediction reaches the 1-5% level, depending on the cut on q^2 , while for the higher moments it is larger and of about 10-20%. For a charm mass at the scale of $\bar{m}_c(3\text{ GeV})$ we observe a better behaviour of the perturbative series, with the expected reduction of theoretical uncertainties when including the $\mathcal{O}(\alpha_s^2)$ corrections. We applied our results also to the decay into a tau lepton, and proposed a measurement of $R(X_c)$ using a lower cut on q^2 to enrich the fraction of $B \rightarrow X_c\tau\bar{\nu}_\tau$ events. We provide our results for the q^2 spectrum in electronic form as ancillary files. They can be employed to incorporate the NNLO corrections into global fits of inclusive semileptonic B-decays, in particular to take advantage of the recent measurements of q^2 moments by Belle and Belle II.

Acknowledgements

We thank J. Usovitsch and F. Lange for the help with `Kira` and R. N. Lee for the help with `Libra`. We thank also P. Gambino, R. van Tonder and K. Vos for discussion and correspondence. The work of M.F. is supported by the European Union's Horizon 2020

³The main strategy to improve the q^2 resolution in the Belle II measurement [19] can not be applied to semitauonic decays as it depends on the presence of exactly one neutrino in the event.

research and innovation program under the Marie Skłodowska-Curie grant agreement No. 101065445 – PHOBIDE. This research was supported in part by the Swiss National Science Foundation (SNF) under contract 200021-212729.

References

- [1] BABAR collaboration, *Measurement of the electron energy spectrum and its moments in inclusive $B \rightarrow X e \nu$ decays*, *Phys. Rev. D* **69** (2004) 111104 [hep-ex/0403030].
- [2] BABAR collaboration, *Measurement and interpretation of moments in inclusive semileptonic decays $\overline{B} \rightarrow X_c l^- \bar{\nu}_l$* , *Phys. Rev. D* **81** (2010) 032003 [0908.0415].
- [3] BELLE collaboration, *Moments of the electron energy spectrum and partial branching fraction of $B \rightarrow X_c e \nu$ decays at Belle*, *Phys. Rev. D* **75** (2007) 032001 [hep-ex/0610012].
- [4] BELLE collaboration, *Moments of the Hadronic Invariant Mass Spectrum in $B \rightarrow X_c \ell \nu$ Decays at BELLE*, *Phys. Rev. D* **75** (2007) 032005 [hep-ex/0611044].
- [5] CLEO collaboration, *Moments of the B meson inclusive semileptonic decay rate using neutrino reconstruction*, *Phys. Rev. D* **70** (2004) 032002 [hep-ex/0403052].
- [6] CDF collaboration, *Measurement of the moments of the hadronic invariant mass distribution in semileptonic B decays*, *Phys. Rev. D* **71** (2005) 051103 [hep-ex/0502003].
- [7] DELPHI collaboration, *Determination of heavy quark non-perturbative parameters from spectral moments in semileptonic B decays*, *Eur. Phys. J. C* **45** (2006) 35 [hep-ex/0510024].
- [8] A. Alberti, P. Gambino, K. J. Healey and S. Nandi, *Precision Determination of the Cabibbo-Kobayashi-Maskawa Element V_{cb}* , *Phys. Rev. Lett.* **114** (2015) 061802 [1411.6560].
- [9] M. Bordone, B. Capdevila and P. Gambino, *Three loop calculations and inclusive V_{cb}* , *Phys. Lett. B* **822** (2021) 136679 [2107.00604].
- [10] G. Finauri and P. Gambino, *The q^2 moments in inclusive semileptonic B decays*, 2310.20324.
- [11] A. Lenz, M. L. Piscopo and A. V. Rusov, *Disintegration of beauty: a precision study*, *JHEP* **01** (2023) 004 [2208.02643].
- [12] J. Albrecht, F. Bernlochner, A. Lenz and A. Rusov, *Lifetimes of b-hadrons and mixing of neutral B-mesons: theoretical and experimental status*, 2402.04224.

- [13] T. Huber, T. Hurth, J. Jenkins, E. Lunghi, Q. Qin and K. K. Vos, *Long distance effects in inclusive rare B decays and phenomenology of $\bar{B} \rightarrow X_d \ell^+ \ell^-$* , *JHEP* **10** (2019) 228 [1908.07507].
- [14] T. Huber, T. Hurth, J. Jenkins, E. Lunghi, Q. Qin and K. K. Vos, *Phenomenology of inclusive $\bar{B} \rightarrow X_s \ell^+ \ell^-$ for the Belle II era*, *JHEP* **10** (2020) 088 [2007.04191].
- [15] M. Fael, T. Mannel and K. Keri Vos, *V_{cb} determination from inclusive $b \rightarrow c$ decays: an alternative method*, *JHEP* **02** (2019) 177 [1812.07472].
- [16] T. Mannel and K. K. Vos, *Reparametrization Invariance and Partial Re-Summations of the Heavy Quark Expansion*, *JHEP* **06** (2018) 115 [1802.09409].
- [17] F. Bernlochner, M. Fael, K. Olschewsky, E. Persson, R. van Tonder, K. K. Vos et al., *First extraction of inclusive V_{cb} from q^2 moments*, 2205.10274.
- [18] BELLE collaboration, *Measurements of q^2 Moments of Inclusive $B \rightarrow X_c \ell^+ \nu_\ell$ Decays with Hadronic Tagging*, *Phys. Rev. D* **104** (2021) 112011 [2109.01685].
- [19] BELLE-II collaboration, *Measurement of lepton mass squared moments in $B \rightarrow X_c \ell \nu$ decays with the Belle II experiment*, *Phys. Rev. D* **107** (2023) 072002 [2205.06372].
- [20] T. Mannel, I. S. Milutin and K. K. Vos, *Inclusive Semileptonic $b \rightarrow c \bar{\nu}$ Decays to Order $1/m_b^5$* , 2311.12002.
- [21] M. Jezabek and J. H. Kuhn, *QCD Corrections to Semileptonic Decays of Heavy Quarks*, *Nucl. Phys. B* **314** (1989) 1.
- [22] M. Jezabek and L. Motyka, *Tau lepton distributions in semileptonic B decays*, *Nucl. Phys. B* **501** (1997) 207 [hep-ph/9701358].
- [23] V. Aquila, P. Gambino, G. Ridolfi and N. Uraltsev, *Perturbative corrections to semileptonic b decay distributions*, *Nucl. Phys. B* **719** (2005) 77 [hep-ph/0503083].
- [24] T. Becher, H. Boos and E. Lunghi, *Kinetic corrections to $B \rightarrow X_c \ell \bar{\nu}$ at one loop*, *JHEP* **12** (2007) 062 [0708.0855].
- [25] A. Alberti, T. Ewerth, P. Gambino and S. Nandi, *Kinetic operator effects in $\bar{B} \rightarrow X_c \ell \nu$ at $O(\alpha_s)$* , *Nucl. Phys. B* **870** (2013) 16 [1212.5082].
- [26] A. Alberti, P. Gambino and S. Nandi, *Perturbative corrections to power suppressed effects in semileptonic B decays*, *JHEP* **01** (2014) 147 [1311.7381].
- [27] T. Mannel, D. Moreno and A. A. Pivovarov, *NLO QCD corrections to inclusive $b \rightarrow c \bar{\nu}$ decay spectra up to $1/m_Q^3$* , *Phys. Rev. D* **105** (2022) 054033 [2112.03875].
- [28] K. Melnikov, *$O(\alpha_s^2)$ corrections to semileptonic decay $b \rightarrow c \bar{\nu}_l$* , *Phys. Lett. B* **666** (2008) 336 [0803.0951].

- [29] S. Biswas and K. Melnikov, *Second order QCD corrections to inclusive semileptonic $b \rightarrow X_c l \bar{\nu}_l$ decays with massless and massive lepton*, *JHEP* **02** (2010) 089 [0911.4142].
- [30] A. Czarnecki and K. Melnikov, *Two loop QCD corrections to semileptonic b decays at maximal recoil*, *Phys. Rev. Lett.* **78** (1997) 3630 [hep-ph/9703291].
- [31] A. Czarnecki and K. Melnikov, *Two loop QCD corrections to $b \rightarrow c$ transitions at zero recoil: Analytical results*, *Nucl. Phys. B* **505** (1997) 65 [hep-ph/9703277].
- [32] A. Czarnecki, *Two loop QCD corrections to $b \rightarrow c$ transitions at zero recoil*, *Phys. Rev. Lett.* **76** (1996) 4124 [hep-ph/9603261].
- [33] A. Czarnecki and K. Melnikov, *Two - loop QCD corrections to semileptonic b decays at an intermediate recoil*, *Phys. Rev. D* **59** (1999) 014036 [hep-ph/9804215].
- [34] M. Fael, K. Schönwald and M. Steinhauser, *A first glance to the kinematic moments of $B \rightarrow X_c l \nu$ at third order*, 2205.03410.
- [35] A. B. Goncharov, *Multiple polylogarithms, cyclotomy and modular complexes*, *Math. Res. Lett.* **5** (1998) 497 [1105.2076].
- [36] A. B. Goncharov, *Multiple polylogarithms and mixed Tate motives*, math/0103059.
- [37] T. Mannel, D. Moreno and A. A. Pivovarov, *Master integrals for inclusive weak decays of heavy flavors at next-to-leading order*, *Phys. Rev. D* **104** (2021) 114035 [2104.13080].
- [38] D. Moreno, *NLO QCD corrections to inclusive semitauonic weak decays of heavy hadrons up to $1/m_b^3$* , *Phys. Rev. D* **106** (2022) 114008 [2207.14245].
- [39] C. Anastasiou and K. Melnikov, *Higgs boson production at hadron colliders in NNLO QCD*, *Nucl. Phys. B* **646** (2002) 220 [hep-ph/0207004].
- [40] P. Nogueira, *Automatic Feynman graph generation*, *J. Comput. Phys.* **105** (1993) 279.
- [41] M. Gerlach, F. Herren and M. Lang, *tapir: A tool for topologies, amplitudes, partial fraction decomposition and input for reductions*, *Comput. Phys. Commun.* **282** (2023) 108544 [2201.05618].
- [42] T. Seidensticker, *Automatic application of successive asymptotic expansions of Feynman diagrams*, in *6th International Workshop on New Computing Techniques in Physics Research: Software Engineering, Artificial Intelligence Neural Nets, Genetic Algorithms, Symbolic Algebra, Automatic Calculation*, 5, 1999, hep-ph/9905298.
- [43] J. Kuipers, T. Ueda, J. A. M. Vermaseren and J. Vollinga, *FORM version 4.0*, *Comput. Phys. Commun.* **184** (2013) 1453 [1203.6543].

- [44] A. V. Smirnov and V. A. Smirnov, *How to choose master integrals*, *Nucl. Phys. B* **960** (2020) 115213 [2002.08042].
- [45] J. Usovitsch, *Factorization of denominators in integration-by-parts reductions*, 2002.08173.
- [46] P. Maierhöfer, J. Usovitsch and P. Uwer, *Kira—A Feynman integral reduction program*, *Comput. Phys. Commun.* **230** (2018) 99 [1705.05610].
- [47] J. Klappert, F. Lange, P. Maierhöfer and J. Usovitsch, *Integral reduction with Kira 2.0 and finite field methods*, *Comput. Phys. Commun.* **266** (2021) 108024 [2008.06494].
- [48] R. H. Lewis, “Computer algebra system fermat.” <https://home.bway.net/lewis>.
- [49] A. V. Kotikov, *Differential equations method: New technique for massive Feynman diagrams calculation*, *Phys. Lett. B* **254** (1991) 158.
- [50] T. Gehrmann and E. Remiddi, *Differential equations for two loop four point functions*, *Nucl. Phys. B* **580** (2000) 485 [hep-ph/9912329].
- [51] J. M. Henn, *Multiloop integrals in dimensional regularization made simple*, *Phys. Rev. Lett.* **110** (2013) 251601 [1304.1806].
- [52] M. Egner, M. Fael, K. Schönwald and M. Steinhauser, *Revisiting semileptonic B meson decays at next-to-next-to-leading order*, *JHEP* **09** (2023) 112 [2308.01346].
- [53] R. N. Lee, *Libra: A package for transformation of differential systems for multiloop integrals*, *Comput. Phys. Commun.* **267** (2021) 108058 [2012.00279].
- [54] R. N. Lee, *Reducing differential equations for multiloop master integrals*, *JHEP* **04** (2015) 108 [1411.0911].
- [55] R. N. Lee, “Fermatica.” <https://github.com/rnlg/Fermatica>.
- [56] X. Liu, Y.-Q. Ma and C.-Y. Wang, *A Systematic and Efficient Method to Compute Multi-loop Master Integrals*, *Phys. Lett. B* **779** (2018) 353 [1711.09572].
- [57] X. Liu and Y.-Q. Ma, *Multiloop corrections for collider processes using auxiliary mass flow*, *Phys. Rev. D* **105** (2022) L051503 [2107.01864].
- [58] X. Liu and Y.-Q. Ma, *AMFlow: A Mathematica package for Feynman integrals computation via auxiliary mass flow*, *Comput. Phys. Commun.* **283** (2023) 108565 [2201.11669].
- [59] H. R. P. Ferguson, D. H. Bailey and S. Arno, *Analysis of pslq, an integer relation finding algorithm*, *Mathematics of Computation* **68** (1999) 351.

- [60] K. Melnikov and T. van Ritbergen, *The Three loop on-shell renormalization of QCD and QED*, *Nucl. Phys. B* **591** (2000) 515 [[hep-ph/0005131](#)].
- [61] K. G. Chetyrkin, *Four-loop renormalization of QCD: Full set of renormalization constants and anomalous dimensions*, *Nucl. Phys. B* **710** (2005) 499 [[hep-ph/0405193](#)].
- [62] P. Marquard, A. V. Smirnov, V. A. Smirnov, M. Steinhauser and D. Wellmann, *$\overline{\text{MS}}$ -on-shell quark mass relation up to four loops in QCD and a general $SU(N)$ gauge group*, *Phys. Rev. D* **94** (2016) 074025 [[1606.06754](#)].
- [63] P. Marquard, A. V. Smirnov, V. A. Smirnov and M. Steinhauser, *Four-loop wave function renormalization in QCD and QED*, *Phys. Rev. D* **97** (2018) 054032 [[1801.08292](#)].
- [64] M. Fael, K. Schönwald and M. Steinhauser, *Relation between the $\overline{\text{MS}}$ and the kinetic mass of heavy quarks*, *Phys. Rev. D* **103** (2021) 014005 [[2011.11655](#)].
- [65] C. W. Bauer, A. Frink and R. Kreckel, *Introduction to the GiNaC framework for symbolic computation within the C++ programming language*, *J. Symb. Comput.* **33** (2002) 1 [[cs/0004015](#)].
- [66] C. Duhr and F. Dulat, *PolyLogTools — polylogs for the masses*, *JHEP* **08** (2019) 135 [[1904.07279](#)].
- [67] M. Fael and F. Herren, “Supplementary material for “NNLO QCD corrections to the q_2 spectrum of inclusive semileptonic B-meson decays”.”
<https://doi.org/10.5281/zenodo.10781498>.
- [68] P. Gambino and C. Schwanda, *Inclusive semileptonic fits, heavy quark masses, and V_{cb}* , *Phys. Rev. D* **89** (2014) 014022 [[1307.4551](#)].
- [69] I. I. Y. Bigi, M. A. Shifman, N. Uraltsev and A. I. Vainshtein, *High power n of m_b in beauty widths and $n = 5 \rightarrow \infty$ limit*, *Phys. Rev. D* **56** (1997) 4017 [[hep-ph/9704245](#)].
- [70] A. Czarnecki, K. Melnikov and N. Uraltsev, *NonAbelian dipole radiation and the heavy quark expansion*, *Phys. Rev. Lett.* **80** (1998) 3189 [[hep-ph/9708372](#)].
- [71] M. Fael, K. Schönwald and M. Steinhauser, *Kinetic Heavy Quark Mass to Three Loops*, *Phys. Rev. Lett.* **125** (2020) 052003 [[2005.06487](#)].
- [72] D. Benson, I. I. Bigi, T. Mannel and N. Uraltsev, *Imprecated, yet impeccable: On the theoretical evaluation of $\Gamma(B \rightarrow X_c l \nu)$* , *Nucl. Phys. B* **665** (2003) 367 [[hep-ph/0302262](#)].
- [73] S. J. Brodsky, G. P. Lepage and P. B. Mackenzie, *On the Elimination of Scale Ambiguities in Perturbative Quantum Chromodynamics*, *Phys. Rev. D* **28** (1983) 228.

- [74] BELLE-II collaboration, *First measurement of $R(X_{\tau/\ell})$ as an inclusive test of the $b \rightarrow c\tau\nu$ anomaly*, 2311.07248.
- [75] E. J. Gustafson, F. Herren, R. S. Van de Water, R. van Tonder and M. L. Wagman, *A model independent description of $B \rightarrow D\pi\ell\nu$ decays*, 2311.00864.
- [76] F. Herren, *The forward-backward asymmetry and differences of partial moments in inclusive semileptonic B decays*, *SciPost Phys.* **14** (2023) 020 [2205.03427].